ACS APPLIED MATERIALS & INTERFACES

Research Article

www.acsami.org

In Situ Determination of the Liquid/Solid Interface Thickness and Composition for the Li Ion Cathode $LiMn_{1.5}Ni_{0.5}O_4$

James F. Browning,[†,⊥] Loïc Baggetto,[‡,⊥] Katherine L. Jungjohann,[§] Yongqiang Wang,[∥] Wyatt E. Tenhaeff,[‡] Jong K. Keum,[†] David L. Wood, III,[‡] and Gabriel M. Veith*[,‡,⊥]

[†]Chemical and Engineering Materials Division and [‡]Materials Science and Technology Division, Oak Ridge National Laboratory, Oak Ridge Tennessee 37831, United States

[§]Center for Integrated Nanotechnologies, Sandia National Laboratories, Albuquerque, New Mexico 87185, United States

[∥]Materials Science and Technology Division, Los Alamos National Laboratory, Los Alamos New Mexico 87545, United States

Supporting Information

ABSTRACT: Using neutron reflectometry, we have determined the thickness and scattering length density profile of the electrode−electrolyte interface for the high-voltage cathode $LiMn_{1.5}Ni_{0.5}O_4$ in situ at open circuit voltage and fully delithiated. Upon exposure to a liquid electrolyte, a thin 3.3 nm Li-rich interface forms due to the ordering of the electrolyte on the cathode surface. This interface changes in composition, as evident by an increase in the scattering length density of the new layer, with charging as the condensed layer evolves from being lithium rich to one containing a much higher concentration of F from the $LiPF_6$ salt. These results show the surface chemistry evolves as a function of the potential.

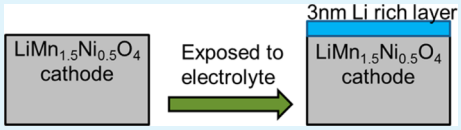

KEYWORDS: *liquid−solid interface, Li ion batteries, SEI layer, in situ battery, neutron reflectometry*

INTRODUCTION

Understanding the chemistry and structure of the liquid−solid interface is a critical challenge to many energy production, storage, and conversion technologies as well as numerous biomedical and chemical processes. For example, this interface controls the corrosion of materials used to generate electricity or store molecules, photocatalytic activity of materials such as TiO_2, biocompatibility of membranes and polymers, and electrochemical energy storage reliability and cyclability. To date, most models of the solid−liquid interface have been based on electrochemical double layers formed under aqueous conditions which fail to capture the complexity of aprotic or nonpolar solvents[1] such as those used in lithium ion batteries. Determining these interfacial structures in situ is challenging due to the large volume of the liquid phase relative to the fraction of molecule species at the interface. This large volume of liquid attenuates or blocks spectroscopic signals from optical methods and prevents the use of classic ultra-high-vacuum surface science methods.[2]

In the case of batteries, reactions between a solid electrode and a liquid electrolyte lead to the formation of the solid electrolyte interphase (SEI), which directly mediates the stability, cycling rate, durability, and safety of the cell.[3−5] The SEI reactions occur on both the anode and cathode and are very similar chemically; however, the importance and fraction of each reaction type differ depending on the electrode surface, state of charge, temperature, and electrolyte composition.[6] Using the most typical electrolyte ($LiPF_6$:ethylene carbonate/dimethyl carbonate (EC/DMC)), several reactions are typically observed on $LiMn_{1.5}Ni_{0.5}O_4$ electrodes like the one used in this study.[7] One reaction involves the salt $LiPF_6$, which decomposes to PF_5 and LiF. PF_5 further reacts with residual water to form HF- and POF_3-type species. The residual water comes from impurities in the electrolyte or persistent adsorbed water on the electrode surface that cannot be removed by simple drying processes.[8] These F species are confined to the electrode surface, forming part of the SEI layer. In addition to the Li salt, EC/DMC can react at the high-potential electrode surface where they decompose to form alkyl carbonates, commonly described as $Li−ROCO_2$, and similar analogues.

Regardless of the complex chemistry, the composition and density of this SEI layer mediate ion diffusion and long-term cyclability. Furthermore, the extent of reaction consumes electrochemically vital Li ions from the cathode, reducing the total fraction of Li available for cycling. Our lack of understanding of this interface prevents us from accurately modeling transport phenomena as well as predicting more stable electrolytes for electrochemical cells, which is critical to designing better batteries.[5,9] Information about battery interfaces is usually obtained after disassembly of the cell and analysis of the surfaces ex situ using standard analytical methods such as infrared spectroscopy and X-ray photoelectron spectroscopy (XPS).[2,10−12] Ex situ analyses can be subject to artifacts as they require either washing the electrode with a solvent or otherwise accounting for any residual electrolyte. This washing may have the disadvantage of removing various components of the SEI layer, effectively giving a partial picture of the SEI chemistry and structure.

Received: May 23, 2014
Accepted: October 6, 2014
Published: October 6, 2014

We describe an approach to probe in situ the liquid−solid interface of a high-voltage Li ion cathode material using neutron reflectometry (NR) and present the experimentally determined thickness and scattering length density (SLD) of this interface as a function of charge. In NR, the specular reflection of neutrons from an interface is measured as a function of the wave vector transfer, $Q = [4\pi \sin(\theta)]/\lambda$, perpendicular to the sample surface. Here, θ is the angle of incidence of the incoming neutron beam with the sample surface and λ the wavelength of the neutron.

Neutrons, by virtue of having no net charge, are deeply penetrating and are therefore ideally suited as a probe to study materials in complicated environments, such as electrochemical cells. Unlike X-rays, neutrons interact with the nuclear potential of atoms and are sensitive to light elements, particularly Li and H. Neutrons are also sensitive to isotopic differences, allowing for selective contrast variation in the design of experiments. For instance, ^{6}Li and ^{7}Li differ in the sign of their SLDs and magnitude of their absorption cross section; this difference can be exploited in studying the exchange of Li during cycling to study the diffusion of Li through the SEI layer.[13]

While recent in situ studies have been reported using nuclear magnetic resonance methods, they still suffer from a lack of depth resolution and involve complicated cell design.[14] In situ X-ray methods are sensitive to volume changes, such as during Li cycling, but are insensitive to low-Z materials such as H and Li which make up a large fraction of the SEI layer.[15] The NR approach detailed below could be applied to all types of electrochemical cells to study SEI formation as well as reaction mechanisms in new battery chemistries, e.g., Li−air. Owejan et al. has recently reported the use of NR to study SEI formation over a Cu current collector without Li intercalation,[16] and Jerliu et al. reported the first investigation of a Li-ion anode (Si).[17] Wang et al. reported the ability to measure Si volume changes with cycling but did not investigate the SEI layer or report electrochemical data.[18] Hirayama et al. reported the first investigation of a cathode ($LiFePO_4$) using NR and found an interesting 20 nm thick layer that forms at the electrode/electrolyte interface which was attributed to a concentration gradient due to double layer formation.[19] Note the charged potential of $LiFePO_4$ is much lower than that of $LiMn_{1.5}Ni_{0.5}O_4$ used in this study, so there should be little to no electrolyte decomposition. While X-ray reflectometry has been applied to investigate the bulk structure of $LiMn_2O_4$, $LiCoO_2$, and $LiFePO_4$ electrodes, NR is more applicable to the characterization of the interfaces of the electrodes.[20−23]

EXPERIMENTAL SECTION

The electrodes were grown through multistep processes based on magnetron sputtering as discussed previously.[24] The starting lithium manganese nickel oxide (LMNO) powder used to prepare the LMNO sputtering target was prepared using a two-step solid-state reaction, as described by Hagh et al.[25] In brief, MnO_2 and NiO (Alfa Aesar) were mixed with a Mn/Ni molar ratio of 3. The mixture was ball-milled for 1 h, recovered, pressed, and fired at 900 °C for 5 h to form a $Ni_{2/3}Mn_2O_4$ spinel phase. Next, the pellet was ground and mixed with the appropriate amount of Li_2CO_3. The mixing was followed by another ball-milling and pressing sequence and a final firing. This firing was achieved at 1000 °C for 15 h followed by a slow cooling of 0.5 °C/min to 700 °C, which was maintained for 40 h, and a final cooling to room temperature at 0.5 °C/min.

The following method was used for electrode fabrication: A 50 mm diameter polished Si wafer was coated with a 10 nm Ti/TiO_2 adhesion layer followed by a 20 nm Pt current collector and a 90 nm Li−Mn−Ni−O electrode by magnetron sputtering of commercially available targets (Ti, Pt) or the homemade LMNO target and subsequently annealed at 550 °C for 20 min in air. The Ti (Kurt J. Lesker) and Pt (Refining Systems, Las Vegas, Nevada) targets were used as-received. In-house sputtering systems capable of a base pressure of at least 10^{-6} Torr were used. The silicon wafers were obtained from the Institute of Electronic Materials Technology, Warszawa, Poland.

Supplementary samples were prepared for electron microscopy imaging using focused ion beam (FIB) extraction from a region of the multilayered film sample coated with Au and Pt protective layers. Aberration-corrected scanning transmission electron microscopy (STEM) was performed on a 200 kV FEI ChemiSTEM equipped with an energy-dispersive X-ray spectrometry (EDS) system operating with silicon drift detectors (SDDs) with a large collection angle (0.7 str). An electron beam current of 164 pA was used to scan pixel areas of 200 × 200 with minimal drift over the 10 min collection interval.

Rutherford backscattering spectrometry (RBS) was performed to examine elemental diffusions between interfaces on the same batch of samples used for the STEM studies. A 3 MeV $^{4}He^{+}$ analyzing beam was generated using an NEC 3 MV Pelletron tandem accelerator at the Ion Beam Materials Laboratory at Los Alamos National Laboratory. Two PIPS particle detectors were used in the measurements: one located at a scattering angle of 167° (Cornell geometry) and the second one located at a scattering angle of 90° (IBM geometry) from the beam direction. The sample normal was tilted 15° from the incident beam, and the accumulated charge was 15 μC for $Pt/TiO_x/Si$ films and 30 μC for $LMNO/Pt/TiO_x/Si$ films with a beam current of ∼10 nA.

X-ray photoelectron spectroscopy was obtained using a PHI 3056 spectrometer with an Al anode source operated at 15 kV and an applied power of 350 W. High-resolution spectroscopy data were collected using a 23.5 eV pass energy; lower resolution survey scans were collected at a pass energy of 93.5 eV. The primary C 1s peak was fixed at 284.8 eV; however, there was no evidence of sample charging.

Electrochemical measurements were performed using a Gamry PCI4 potentiostat using the setup represented in Figure S6 (Supporting Information). Cells were assembled under He in a glovebag, at the beamline, prior to experiments to minimize air and moisture exposure. The electrochemical cell was constructed using single-crystal Si substrates for the electrodes separated by a Teflon-coated Viton gasket with a 1 mm cross-sectional diameter. The total cell volume is approximately 3 mL. The cell was charged at a maximum current of 9 mA to 4.75 V and held at that potential during the measurement. NR experiments were started after a 1/2 h of charge. NR measurements were carried out on the Liquids Reflectometer (BL-4B) at the Spallation Neutron Source (SNS) at Oak Ridge National Laboratory. The Liquids Reflectometer is a horizontal geometry instrument using the time-of-flight technique with neutrons of wavelength 2.5−17.5 Å with an effective single bandwidth of 3.5 Å at an accelerator pulse frequency of 60 Hz. For these measurements a single-wavelength band centered at 4.25 Å, together with seven incidence angles (θ = 0.2°, 0.27°, 0.34°, 0.48°, 0.6 2°, 1.12°, and 2.01°), provided a wave vector transfer (Q_z) range extending from 0.005 to 0.16 $Å^{-1}$. An incidence beam slit was adjusted for each incident angle to maintain a constant beam profile on the sample. Analysis of the specularly reflected neutron data was carried out using the computer modeling and fitting program NRFit developed by Cho et al.[26] The program uses the Parratt formalism[27] to calculate reflectivity from a model SLD profile for comparison to the experimentally acquired NR data.

RESULTS AND DISCUSSION

Structure and Growth of the Working Electrode. The LMNO electrode material used in this work was slightly Li rich, leading to the inclusion of a small concentration of Li_2MnO_3 and $LiMn_xNi_{1-x}O_2$ along with the majority LMNO phase.[24] The working electrode structure required for these studies is complicated due to ion diffusion between the layers. Initially, model parameters representing the electrode structure used to

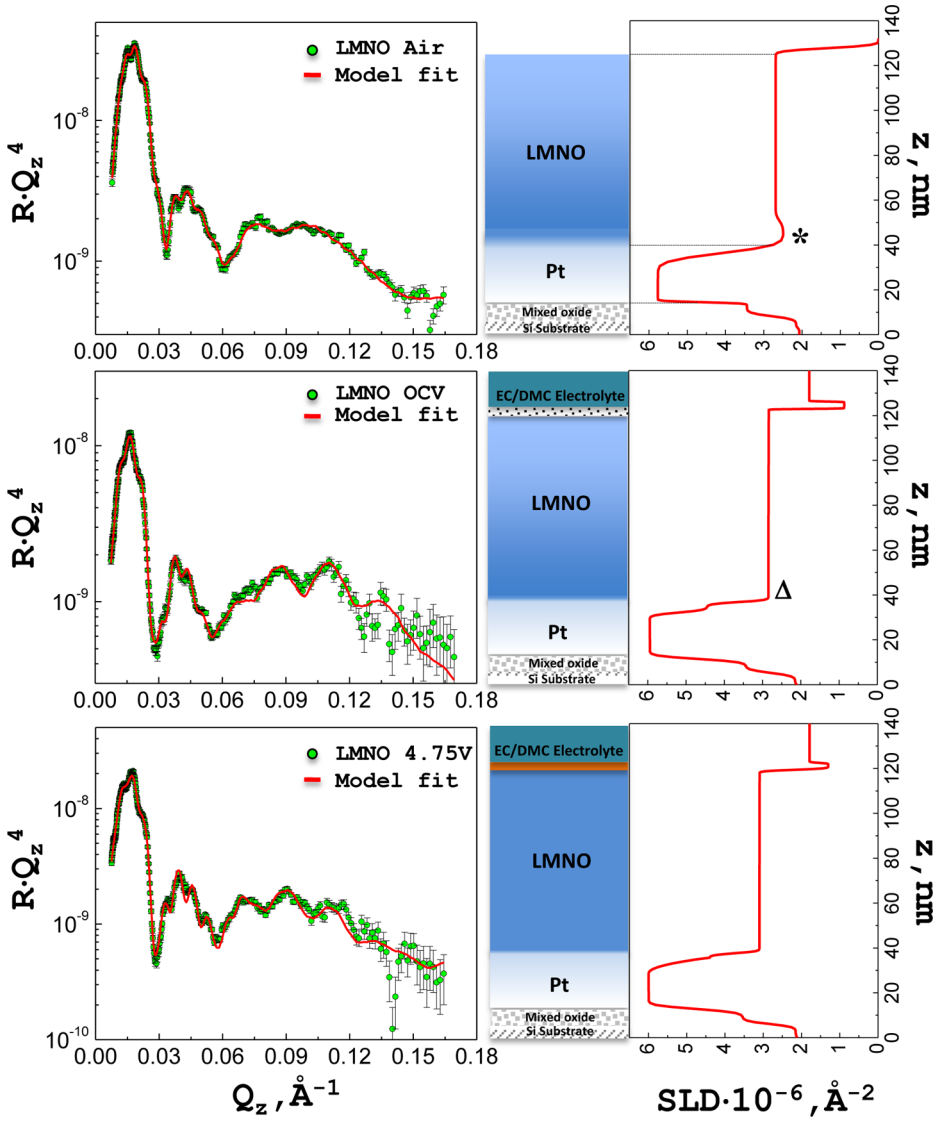

Figure 1. Reflectivity profiles collected in situ for the LMNO film (a, top left) in air, (c, middle left) at the OCV, and (e, bottom left) charged to 4.75 V. Corresponding SLD plots representing the film thickness (b, top right; d, middle right; f, bottom right). The schematics in the middle represent the layers formed from the silicon substrate out.

fit the reflectivity data were input from deposition parameters measured from a quartz crystal microbalance and adjusted manually to yield a reasonable representation of the data. Interfacial regions separating individual layers within the profile were modeled using an error function distribution representing interfacial roughness and/or diffuseness. Subsequently, select model parameters were allowed to vary until a best fit to the data, using a Levenberg−Marquardt algorithm, was obtained as determined by a reduced χ^2 value. To improve the confidence in our resulting fits to the NR data and to validate our model for the annealed sample measured in air, STEM and RBS experiments were performed on samples produced in a separate deposition run, but under conditions similar to those of the NR sample. XPS was also performed on these witness samples to understand the as-prepared surface chemistry.

The reflectivity profile of the as-prepared annealed electrode thin film assembly, presented in Figure 1a, was collected in air, where the neutrons entered from the air−LMNO interface and reflected off the surface onto a 2-D detector. The green, circular data points represent the measured reflectivity profile, while the red, solid line represents the best fit to the data determined by the SLD profile shown in the plot to the right (Figure 1b) and summarized in Table S1 (Supporting Information). The data are plotted as RQ^4 vs Q to highlight salient features of the reflectivity profile and the quality of the fit derived from the SLD model. The SLD profile represents the compositional and density variation comprising material layers normal to the film surface and can be represented mathematically by $\beta(z) = \sum_i b_i n_i$, where b_i is the coherent neutron scattering length and n_i the nuclear number density of a given atomic species at depth z within the layer. Initially, a four-layer model was used to fit the data on the basis of the deposition of the Ti/TiO_x wetting layer, followed by Pt and LMNO, onto the native oxide of the silicon substrate. It was found that the four-layer model did not sufficiently represent the data, so an additional layer was added, first to the surface of the LMNO and then to the LMNO/Pt interfacial region. The best fit (χ^2 = 2.6) was achieved by the addition of a layer at the LMNO/Pt interface, indicating an interaction between the Pt and LMNO during the deposition and/or annealing steps.

The Ti/TiO_x wetting layer between Pt and the Si substrate was found to have a total thickness of ~11 nm. The layer is comprised of two regions, with the thicker and higher SLD region being closest to the Pt layer. This region in the SLD profile suggests an intermixing of Pt and TiO_x at the interface closest to the substrate with a thin TiO_x/SiO_x layer separating it from the Si substrate. No evidence of a pure Ti layer is seen in the profile. Figure 2 shows the RBS data collected for the Si/

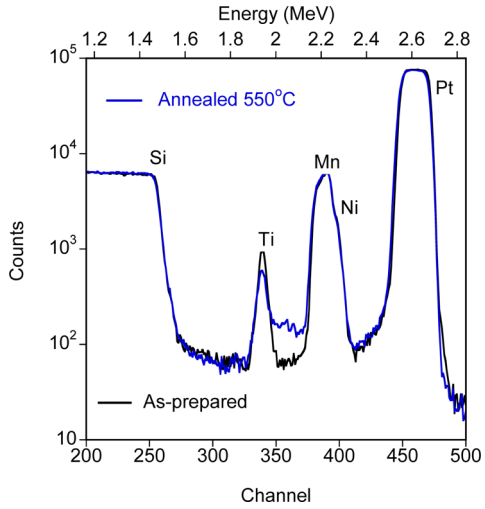

Figure 2. RBS data collected for an as-prepared LMNO witness sample (black) and the same witness sample annealed at 550 °C in air (blue).

TiO_x/Pt/LMNO witness sample before and after annealing. These data clearly show a reduction/broadening in the Ti peak intensity along with a shift to the Pt interface with annealing consistent with Ti diffusion into the Pt layer. Similar trends are observed for a Si/TiO_x/Pt stack, Figure S1 (Supporting Information), confirming that this Ti diffusion is intrinsic to the Ti−Pt chemistry. Similar results have been reported by Aspelmeyer et al. for a 100 nm Pt film deposited on 10 nm Ti on a SiO_x/Si substrate and then annealed at 650 °C in O_2, resulting in a volume fraction of 0.30 Ti/TiO_x within the Pt film.[28] This result is also consistent with the findings of Yao et al.[28,29]

From the NR data, the Pt layer thickness was found to be 21.8 nm with an SLD less than that expected for pure Pt (the theoretical SLD of Pt is 6.35×10^{-6} Å^{-2}).[30] A measured value of 5.77×10^{-6} Å^{-2} represents an approximate 10% decrease in the SLD of Pt. It is not unusual for the mass density of a thin metal film to fall below that expected for bulk materials. Reasons for this discrepancy include a high concentration of grain boundaries or the presence of voids or other defect structures within the layer such as oxide inclusions. However, a 10% lower SLD compared to that expected for Pt is somewhat puzzling and thought to be due to the presence of Li and/or Ti within the layer. Both Li and Ti have negative SLDs requiring only modest amounts to lower the overall SLD of the layer. In this case a volume fraction of 0.08 or 0.07, respectively, would be required; Pt can be lithiated up to $Li_{4.4}Pt$. The RBS data support the conclusion of elemental diffusion from the LMNO layer, Figure 2. There are small, but observable changes in the Pt layer closest to the LMNO, Figure 2, that are not observed for the Si/TiO_x/Pt stack, Figure S1 (Supporting Information), consistent with some Li diffusing into the Pt layer. Li may be forced into the current collector due to the plasma potential or postannealing treatment. This slight lithiation does not affect the electronic resistance of the Pt current collector.[24]

At the Pt/LMNO interface there is a slight decrease in the LMNO SLD near the platinum surface. This is likely attributed to the RBS observed increase in titanium concentration and/or lithium or voids at or near the Pt interface. The thickness of this interfacial zone was measured at 14.5 nm, by NR, and shows an approximate 5% decrease in SLD relative to the "bulk" of the LMNO layer. The interfacial roughness between LMNO and Pt was 3.8 nm, indicating a rough or diffuse interface between the layers. Electron microscopy data, collected on the same sample used for RBS, support this model of the Pt/LMNO interface. Indeed, as observed in Figures 3 and S2 (Supporting

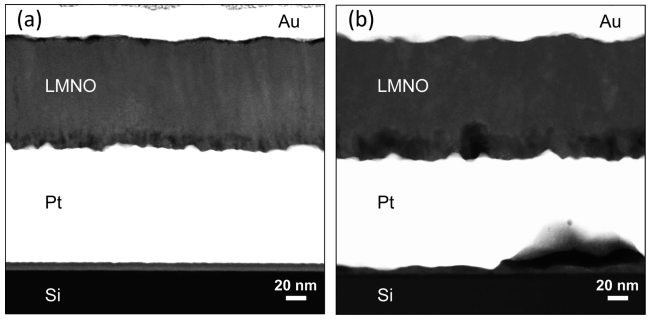

Figure 3. High-angle annular dark-field STEM images of (a) unannealed and (b) annealed multilayer film samples. Layers from the bottom up are composed of Si with a thin oxide surface layer, TiO_2, Pt, and LiMnNiO, coated with a Au sputtered film. Pt interfaces have been roughened by the annealing process, forming voids or concentrated Li regions on the LMNO side.

Information), after deposition (left) and especially after annealing (right), large voids or regions consisting of species with low atomic numbers are evident. Energy-dispersive X-ray mapping of this interface and higher resolution imaging, Figures 4 and S3 and S4 (Supporting Information) confirm the interdiffusion of Pt and LMNO at this interface. Furthermore, these TEM data confirm the refined thicknesses of 14.5 nm for the interfacial zone described above. In addition, we observe a surface roughness of about 4 nm, consistent with the NR fits. This roughness likely comes from film stresses or void structure observed in the microscopy data.

Using this five-layer model, the total thickness of the LMNO layer was found to be 91.5 nm, in good agreement with the predicted film thickness controlled by varying the deposition conditions. The weighted average SLD of the LMNO layer (including the interfacial region between the LMNO and Pt, which was determined to have a slightly lower SLD from the fit) was found to be ~2.64×10^{-6} Å^{-2} (a theoretical value of 3.02×10^{-6} Å^{-2} would be expected assuming a dense stoichiometric film) and shows a decrease near the interface closest to the platinum current collector (marked with an asterisk). The lower measured SLD, versus theoretical LMNO, suggests the LMNO film is Li rich, which is consistent with the electrochemical properties of this electrode as described before[24] and/or would suggest a lower mass density than that predicted. No distinguished surface layer was used to fit the NR profile; data modeled with the addition of a surface layer had a significantly poorer fit, indicating that if a surface layer was present, the neutrons were not sensitive to it (Figure S5, Supporting Information). XPS measurements on the witness

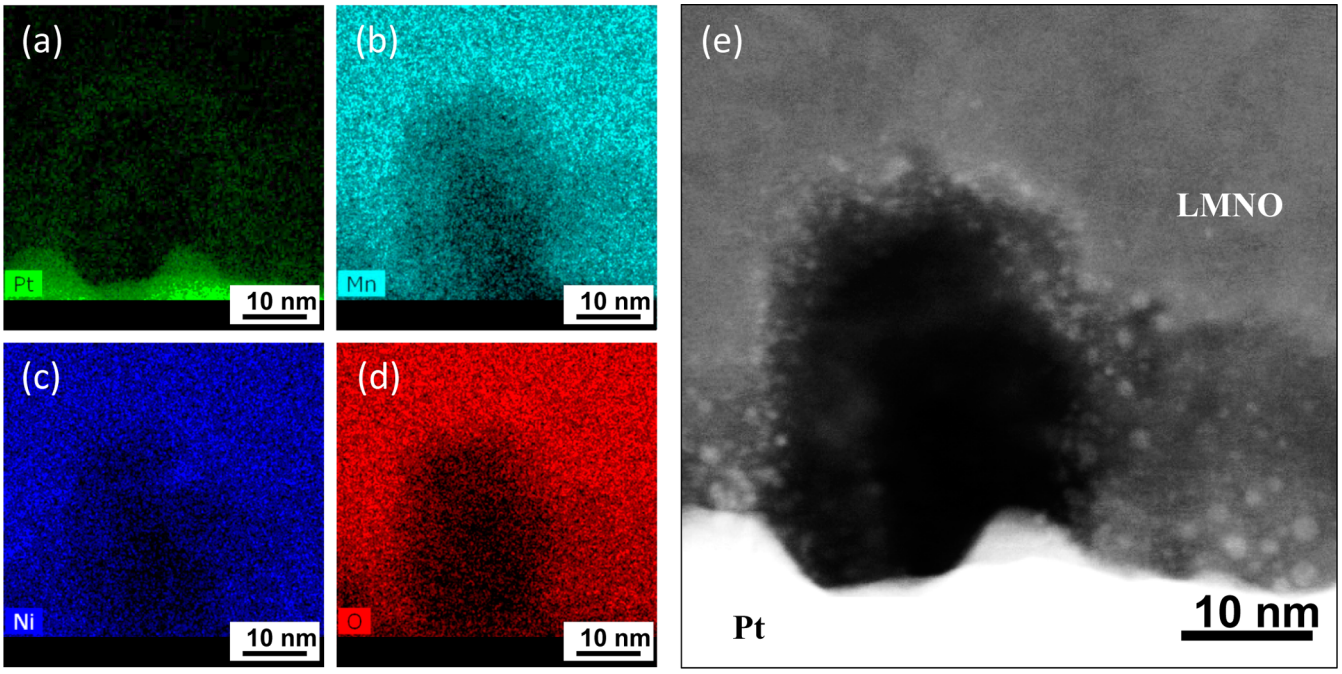

Figure 4. Characteristic X-ray map of the annealed sample at the Pt/LMNO interface of (a) Pt, (b) Mn, (c) Ni, and (d) O. (e) High-angle annular dark-field STEM image of the X-ray map region.

samples indicate that the surface has no excess Li_2CO_3 and only low concentrations of adventitious carbon.

Structure at the Open Circuit Voltage. The LMNO thin film electrode was assembled into an electrochemical cell, Figure S6 (Supporting Information), using the standard 1.2 M $LiPF_6$ ethylene carbonate/dimethyl carbonate (3:7 wt %) electrolyte (Novolyte) and a Pt metal anode deposited onto an opposing Si wafer. The electrolyte had H_2O concentrations of less than 1 ppm as measured using a Karl Fischer titrator. Pt was selected as the anode due to its stability in air. This is a full cell configuration with Pt acting as the anode and the LMNO layer acting as the Li source as opposed to a half-cell configuration. The reflectivity and SLD profiles of the LMNO film when first wetted with electrolyte at the open circuit voltage (OCV; 0.56 V versus Pt counter electrode, full cell configuration) are shown in Figure 1c,d. The reflectivity data are plotted in Figure S7 (Supporting Information) to highlight the changes between the samples, while Figure S8 (Supporting Information) compares the SLD profile in greater detail. In the electrochemical cell, neutrons entered though the side of the Si wafer and reflected from the Si/electrode assembly interface (Figure S6). The analysis of the resulting reflectivity profile was carried out by initially allowing only the parameters associated with the LMNO and Pt layers to vary, i.e., thickness, roughness, and SLD. Subsequently, parameters associated with the TiO_x layer and the SLD of the electrolyte were also allowed to vary to ensure no change with cycling.

While the thickness of the film extending to the Pt surface remains constant, two changes in the overall structure of the film are observed in the SLD profile at the OCV (χ^2 = 2.8). First, a significant change in film structure occurs at the LMNO/Pt interface. The ~14 nm interfacial region near Pt, seen in the film measured in air, narrowed by more than half and shows a 50% increase in SLD. This increase in interfacial SLD, along with the slight decrease observed in the SLD of the LMNO, may indicate the excess Li from the interface has diffused throughout the bulk of the LMNO layer. This interface layer is very thin, and the slight potential applied when the OCV is measured may be enough to drive Li motion (marked with a "Δ").[31] The width and SLD of the remaining interfacial structure at the Pt surface are similar to those seen at the Pt interface nearest to the Si substrate. The presence of TiO_x at each of the Pt interfaces would be consistent with the observations by both Aspelmeyer and Yao.[28,29] The second major change is the formation of a 3.3 nm layer on the surface of the LMNO. The SLD of this surface layer, as determined by the best fit to the data, is 0.87×10^{-6} Å^{-2}. This low SLD is consistent with a Li-rich layer, which likely originates from Li in the $LiPF_6$ salt. Hirayama et al. described a thicker (20 nm) condensed layer at the OCV but did not estimate its composition.[19] Recently, Yu et al. using sum frequency generated spectroscopy found preferential ordering of electrolyte molecules at the cathode surface under open circuit conditions[32] similar to what we observe in our data. This orientation is very likely important for the initial nucleation and growth of the SEI on the electrode surface.

It is important to note that the ability to detect this Li layer is unique to neutrons; such a layer would not be evident to typical X-ray reflectivity measurements due to the low X-ray cross section of Li. The 0.6 nm interfacial roughness indicates that the layer is uniform and may be conformal to the original LMNO surface. This layer is much thinner and uniform than what was described previously[19] and may be unique to electrochemical cells. Extensive efforts to model the data without the layer were unsuccessful. Figure S9 (Supporting Information) demonstrates fits to the reflectometry data using the model described above, a model with no surface layer, and a model with no surface layer but where the SLD of the LMNO was allowed to change. In principle, there are an infinite number of solutions, but the model chosen makes physical sense on the basis of the cell chemistry and the experimental RBS, XPS, and STEM data. Furthermore, even though the data

do not extend to high Q values due to incoherent scatter from the electrolyte, the presence of a thin layer will affect the shape and rate of falloff of the profile over the Q range probed in the measurement. This data analysis further demonstrates the sensitivity of NR to the formation of very thin interface structures in situ and the importance of these studies to understanding battery interfaces. It is important to note that there is very little change in the SLD or thickness of the LMNO layer, indicating that except for the surface reaction the electrode is stable at the OCV. The results of the in situ analysis of the film measured at the OCV are summarized in Table S2 (Supporting Information).

Surface Structure of the Charged Electrode. The electrochemical cycling performance of these electrodes was reported previously.[24] On the basis of this prior work, the working electrodes were charged potentiostatically to 4.75 V (vs Li/Li^+) (Figure S10, Supporting Information). The sample was held at this potential to prevent a spontaneous discharge reaction from occurring related to the reduction of Ni^{4+} to Ni^{3+} and Ni^{2+}. NR measurements were begun when the potential reached 4.75 V vs Li/Li^+ and the current had dropped to <2 mA. After delithiation (charge) a number of important changes occur in the structure of the LMNO film. The reflectivity and SLD profiles of the LMNO film measured at 4.75 V are shown in Figure 1e,f (χ^2 = 3.9). First, the LMNO layer shows an increase of ∼9% in the SLD accompanied by a decrease of 5% in thickness relative to that seen before charging. The increase in SLD is due to the removal of Li from the LMNO layer to form Li-free $Mn_{1.5}Ni_{0.5}O_4$ (MNO); Li has a negative SLD, and upon delithiation the average SLD of the LMNO layer increases to 3.10×10^{-6} $Å^{-2}$ due to absence of Li. The decrease in layer thickness is due to a decrease in the lattice parameter of MNO versus LMNO (6.6 vol % theoretically (8.005 Å versus 8.177 Å))[25] and again indicates a near complete delithiation of the electrode layer. The interfacial region between the LMNO and Pt showed the opposite behavior in that the SLD decreased from 4.49×10^{-6} to 4.4×10^{-6} $Å^{-2}$ with an increase of ∼2 nm in width. Of interest was a noted change in the Pt SLD. The Pt SLD increased from roughly 5.77×10^{-6} to 6.0×10^{-6} $Å^{-2}$, a value within 5% of theoretical value for Pt. This increase in SLD at the charged potential possibly indicates the Li inclusion within the Pt electrode during sample fabrication is subsequently driven out from the layer during charging.

The most notable result of this study was the change in SLD observed for the surface reaction layer with delithiation. There was a 1.5-fold increase in the SLD value to 1.30×10^{-6} $Å^{-2}$, indicating the formation of a well-defined layer. This increase in SLD suggests a significant reduction in Li content at the interface. These results indicate that there is an initial chemical reaction layer or condensed layer formed on the electrode surface. This is likely the precursor phase to SEI formation. Upon charging, this layer reacts, forming a layer with significantly different chemical composition. We believe this is the first observation of the formation of the SEI layer from this precursor layer. Results of the in situ analysis of the film measured after dilithiation of the LMNO layer are summarized in Table S3 (Supporting Information). The changes in the SLD and layer thickness for LMNO and Pt from the measurement in air to the charged state are summarized in Figure S9 (Supporting Information).

Our results clearly show that a dense 3.1 nm film is formed at the surface of the charged electrode. The increase in SLD at the electrode interface is attributed to an increase in materials with high SLD, which could include Pt from the anode or fluorine from the electrolyte and/or the loss of Li. XPS studies could not be performed in a reasonable period of time due to the residual radioactivity of the sample; however, there was no evidence of Pt on the surface, via XPS, after 2 months of storage in air. The XPS studies did show a significant concentration of F on the cathode surface, Figure S11 (Supporting Information), along with polymeric C−O species and P−O from the decomposition of the electrolyte consistent with prior studies.[33,34] Therefore, this increase in SLD is attributed to F (b = 5.65 fm)[30] and P (b = 5.13 fm)[30] solid products on the cathode surface.

CONCLUSION

For the first time, we have experimentally measured the SLD and thickness of the initial SEI layer that forms on a high-voltage cathode during delithiation in situ. The above results indicate the formation of a dense 3.1 nm thick fluorine- and phosphorus-rich reaction layer at 4.75 V on the surface of the LMNO electrode. To unambiguously determine the H content, hydrogen/deuterium studies will be performed to further identify the reaction layer composition. The methodology described above can be applied to numerous electrochemical systems to determine the interface chemistry and the resulting layer thickness. It provides valuable experimental information for the development of interfacial reaction models and to predict more stable electrolyte configurations in the future. Perhaps as important, these results provide experimental validation of the starting SEI structures for computational studies of battery interfaces.

ASSOCIATED CONTENT

Supporting Information

Tables with fits to the data, RBS data, STEM images, EDX mapping, cell schematics, fitting profiles, XPS data, and raw NR data. This material is available free of charge via the Internet at http://pubs.acs.org.

AUTHOR INFORMATION

Corresponding Author

*E-mail: veithgm@ornl.gov. Phone: 865-576-0027.

Author Contributions

⊥J.F.B., L.B., and G.M.V. contributed equally to this work.

Notes

The authors declare no competing financial interest.

ACKNOWLEDGMENTS

This research was supported by the Materials Sciences and Engineering Division, Office of Basic Energy Sciences, U.S. Department of Energy (DOE), under contract with UT-Battelle, LLC (G.M.V.). A portion of this work was sponsored by the Laboratory Directed Research and Development Program of Oak Ridge National Laboratory, managed by UT-Battelle, LLC, for the U.S. DOE (L.B., W.E.T., D.L.W.). Neutron reflectometry measurements were carried out on the liquids reflectometer at the Spallation Neutron Source, which is sponsored by the Scientific User Facilities Division, Office of Basic Energy Sciences, U.S. DOE (J.F.B., J.K.K.). STEM imaging and RBS experiments were performed at the Center for Integrated Nanotechnologies, an Office of Science User Facility operated for the U.S. DOE Office of Science. Sandia

National Laboratories is a multiprogram laboratory operated by Sandia Corp., a wholly owned subsidiary of Lockheed Martin Co., for the U.S. DOE's National Nuclear Security Administration under Contract DE-AC04-94AL85000 (K.L.J.). RBS experiments were performed at the Center for Integrated Nanotechnologies, an Office of Science User Facility operated for the U.S. DOE Office of Science. Los Alamos National Laboratory, an affirmative action equal opportunity employer, is operated by Los Alamos National Security, LLC, for the National Nuclear Security Administration of the U.S. DOE under Contract DE-AC52-06NA25396 (Y.W.).

REFERENCES

(1) Staffan, W. The History of Electrokinetic Phenomena. *Curr. Opin. Colloid Interface Sci.* **2010**, *15*, 119−124.
(2) Zaera, F. Probing Liquid/Solid Interfaces at the Molecular Level. *Chem. Rev.* **2012**, *112*, 2920−2986.
(3) Peled, E. The Electrochemical Behavior of Alkali and Alkaline Earth Metals in Nonaqueous Battery Systems—The Solid Electrolyte Interphase Model. *J. Electrochem. Soc.* **1979**, *126*, 2047−2051.
(4) Peled, E.; Golodnitsky, D.; Ardel, G. Advanced Model for Solid Electrolyte Interphase Electrodes in Liquid and Polymer Electrolytes. *J. Electrochem. Soc.* **1997**, *144*, L208−L210.
(5) Xu, K. Nonaqueous Liquid Electrolytes for Lithium-Based Rechargeable Batteries. *Chem. Rev.* **2004**, *104*, 4303−4418.
(6) Baggetto, L.; Dudney, N. J.; Veith, G. M. Surface Chemistry of Metal Oxide Coated Lithium Manganese Nickel Oxide Thin Film Cathodes Studied by XPS. *Electrochim. Acta* **2013**, *90*, 135−147.
(7) Duncan, H.; Duguay, D.; Abu-Lebdeh, Y.; Davidson, I. J. Study of the $LiMn_{1.5}Ni_{0.5}O_4$/Electrolyte Interface at Room Temperature and 60 °C. *J. Electrochem. Soc.* **2011**, *158*, A537−A545.
(8) Browning, K. L.; Baggetto, L.; Unocic, R. R.; Dudney, N. J.; Veith, G. M. Gas Evolution from Cathode Materials: A Pathway to Solvent Decomposition Concomitant to SEI Formation. *J. Power Sources* **2013**, *239*, 341−346.
(9) Goodenough, J. B.; Kim, Y. Challenges for Rechargeable Li Batteries. *Chem. Mater.* **2010**, *22*, 587−603.
(10) Mai, L.; Dong, Y.; Xu, L.; Han, C. Single Nanowire Electrochemical Devices. *Nano Lett.* **2010**, *10*, 4273−4278.
(11) Huang, J. Y.; Zhong, L.; Wang, C. M.; Sullivan, J. P.; Xu, W.; Zhang, L. Q.; Mao, S. X.; Hudak, N. S.; Liu, X. H.; Subramanian, A.; Fan, H.; Qi, L.; Kushima, A.; Li, J. In Situ Observation of the Electrochemical Lithiation of a Single SnO_2 Nanowire Electrode. *Science* **2010**, *330*, 1515−1520.
(12) Sacci, R. L.; Dudney, N. J.; More, K. L.; Parent, L. R.; Arslan, I.; Browning, N. D.; Unocic, R. R. Direct Visualization of Initial SEI Morphology and Growth Kinetics during Lithium Deposition by in Situ Electrochemical Transmission Electron Microscopy. *Chem. Commun.* **2014**, *50*, 2104−2107.
(13) Bridges, C. A.; Sun, X.-G.; Zhao, J.; Paranthaman, M. P.; Dai, S. In Situ Observation of Solid Electrolyte Interphase Formation in Ordered Mesoporous Hard Carbon by Small-Angle Neutron Scattering. *J. Phys. Chem. C* **2012**, *116*, 7701−7711.
(14) Chandrashekar, S.; Trease, N. M.; Chang, H. J.; Du, L.-S.; Grey, C. P.; Jerschow, A. ^{7}Li MRI of Li Batteries Reveals Location of Microstructural Lithium. *Nat. Mater.* **2012**, *11*, 311−315.
(15) Chattopadhyay, S.; Lipson, A. L.; Karmel, H. J.; Emery, J. D.; Fister, T. T.; Fenter, P. A.; Hersam, M. C.; Bedzyk, M. J. In Situ X-ray Study of the Solid Electrolyte Interphase (SEI) Formation on Graphene as a Model Li-Ion Battery Anode. *Chem. Mater.* **2012**, *24*, 3038−3043.
(16) Owejan, J. E.; Owejan, J. P.; DeCaluwe, S. C.; Dura, J. A. Solid Electrolyte Interphase in Li-Ion Batteries: Evolving Structures Measured in Situ by Neutron Reflectometry. *Chem. Mater.* **2012**, *24*, 2133−2140.
(17) Jerliu, B.; Dorrer, L.; Huger, E.; Borchardt, G.; Steitz, R.; Geckle, U.; Oberst, V.; Bruns, M.; Schneider, O.; Schmidt, H. Neutron Reflectometry Studies on the Lithiation of Amorphous Silicon Electrodes in Lithium-Ion Batteries. *Phys. Chem. Chem. Phys.* **2013**, *15*, 7777−7784.
(18) Wang, H.; Downing, R. G.; Dura, J. A.; Hussey, D. S. In Situ Neutron Techniques for Studying Lithium Ion Batteries. In *Polymers for Energy Storage and Delivery: Polyelectrolytes for Batteries and Fuel Cells*; ACS Symposium Series *1096*; American Chemical Society: Washington, DC, 2011; Chapter 6, pp 91−106.
(19) Hirayama, M.; Yonemura, M.; Suzuki, K.; Torikai, N.; Smith, H.; Watkinsand, E.; Majewski, J.; Kanno, R. Surface Characterization of $LiFePO_4$ Epitaxial Thin Films by X-ray/Neutron Reflectometry. *Denki Kagaku* **2010**, *78*, 413−415.
(20) Dupre, N.; Martin, J. F.; Oliveri, J.; Soudan, P.; Yamada, A.; Kanno, R.; Guyomard, D. Relationship Between Surface Chemistry and Electrochemical Behavior of $LiNi_{1/2}Mn_{1/2}O_2$ Positive Electrode in a Lithium-Ion Battery. *J. Power Sources* **2011**, *196*, 4791−4800.
(21) Hirayama, M.; Ido, H.; Kim, K.; Cho, W.; Tamura, K.; Mizuki, J. i.; Kanno, R. Dynamic Structural Changes at $LiMn_2O_4$/Electrolyte Interface during Lithium Battery Reaction. *J. Am. Chem. Soc.* **2010**, *132*, 15268−15276.
(22) Hirayama, M.; Sakamoto, K.; Hiraide, T.; Mori, D.; Yamada, A.; Kanno, R.; Sonoyama, N.; Tamura, K.; Mizuki, J. i. Characterization of Electrode/Electrolyte Interface Using *in Situ* X-ray Reflectometry and $LiNi_{0.8}Co_{0.2}O_2$ Epitaxial Film Electrode Synthesized by Pulsed Laser Deposition Method. *Electrochim. Acta* **2007**, *53*, 871−881.
(23) Hirayama, M.; Sonoyama, N.; Ito, M.; Minoura, M.; Mori, D.; Yamada, A.; Tamura, K.; Mizuki, J. i.; Kanno, R. Characterization of Electrode/Electrolyte Interface with X-ray Reflectometry and Epitaxial-Film $LiMn_2O_4$ Electrode. *J. Electrochem. Soc.* **2007**, *154*, A1065−A1072.
(24) Baggetto, L.; Unocic, R. R.; Dudney, N. J.; Veith, G. M. Fabrication and Characterization of Li−Mn−Ni−O Sputtered Thin Film High Voltage Cathodes for Li-Ion Batteries. *J. Power Sources* **2012**, *211*, 108−118.
(25) Hagh, N. M.; Amatucci, G. G. A New Solid-State Process for Synthesis of $LiMn_{1.5}Ni_{0.5}O_{4-\delta}$ Spinel. *J. Power Sources* **2010**, *195*, 5005−5012.
(26) Cho, J. H.; Smith, G. S.; Hamilton, W. A. NRFit—A Program for the Simulation and Fitting of Neutron Reflectivity Data. Developed at Oak Ridge National Laboratory, Low-Q Scattering Group, Neutron Scattering Sciences. http://www.igorexchange.com/project/nrfit (accessed Oct 30, 2011), http://sourceforge.net/projects/nrfitproject/ (accessed Oct 12, 2012).
(27) Parratt, L. G. Surface Studies of Solids by Total Reflection of X-Rays. *Phys. Rev.* **1954**, *95*, 359.
(28) Aspelmeyer, M.; Klemradt, U.; Hartner, W.; Bachhofer, H.; Schindler, G. High-Resolution X-ray Reflectivity Study of Thin Layered Pt-Electrodes for Integrated Ferroelectric Devices. *J. Phys. D: Appl. Phys.* **2001**, *34*, A173−178.
(29) Wang, K.; Yao, K.; Chua, S. J. Titanium Diffusion and Residual Stress of Platinum Thin Films on Ti/SiO_2/Si Substrate. *J. Appl. Phys.* **2005**, *98*, 013538.
(30) Sears, V. F. Neutron Scattering Lengths and Cross Sections. *Neutron News* **1992**, *3*, 26−37.
(31) A Fluke 79 multimeter was used in the glovebox to measure the open circuit voltage. This instrument applies about 0.6 mA of current to measure OCV. We used the instrument several times, for a total of 3−4 s, to measure OCV and ensure no shorting within the cell. This corresponds to about 2×10^{-8} mol of current. The 12.3 nm reaction layer contains about 6.1×10^{-7} mol of material assuming a density of 4.5 g/cm^3. This applied current would be enough to move around 3% of the Li in the layer.
(32) Yu, L.; Liu, H.; Wang, Y.; Kuwata, N.; Osawa, M.; Kawamura, J.; Ye, S. Preferential Adsorption of Solvents on the Cathode Surface of Lithium Ion Batteries. *Angew. Chem., Int. Ed.* **2013**, *52*, 5753−5756.
(33) Dedryvere, R.; Foix, D.; Franger, S.; Patoux, S.; Daniel, L.; Gonbeau, D. Electrode/Electrolyte Interface Reactivity in High-Voltage Spinel $LiMn_{1.6}Ni_{0.4}O_4/Li_4Ti_5O_{12}$ Lithium-Ion Battery. *J. Phys. Chem. C* **2010**, *114*, 10999−11008.

(34) Dedryvere, R.; Gireaud, L.; Grugeon, S.; Laruelle, S.; Tarascon, J. M.; Gonbeau, D. Characterization of Lithium Alkyl Carbonates by X-ray Photoelectron Spectroscopy: Experimental and Theoretical Study. *J. Phys. Chem. B* **2005**, *109*, 15868−15875.